PII: S0032-3861(97)10112-4

Polymer Vol. 39 No. 21, pp. 5197–5201, 1998
0032-3861/98/$ – see front matter
© 1998 Elsevier Science Ltd. All rights reserved.

Non-linear spherulite growth and phase change at the spherulite growth front in isotactic polypropylene/partially hydrogenated oligo(styrene-*co*-indene) blend

Chang Hyung Lee
Materials Analysis Division, Department of Chemistry, National Institute of Technology and Quality, 2, Jungang-dong, Kwacheon City, Kyunggi-do 427-010, South Korea
(Received 1 August 1997; accepted 4 September 1997)

In a previous study, an immiscibility loop in the isotactic polypropylene/partially hydrogenated oligo(styrene-*co*-indene) (HSI) blend was found by the cloud point method. Then morphology development both at one phase region outside the loop and at two phases inside the loop was investigated. At temperatures studied, a non-linear growth of the spherulite was observed and it was ascribed to the rejected HSI at the growth front of the spherulite. At one phase region just outside the loop, crystallization preceded, and it induced liquid–liquid phase separation at the trapped region between spherulites. At two phases inside the loop, spinodal decomposition proceeded, the crystallization from the decomposed state followed, and then the crystallization induced the dissolution of the liquid–liquid phase separation at the growth front of the spherulite. This behaviour, phase change from the one phase to the two phases and from the two phases to the one phase, was interpreted by the rejected impurity (HSI) at the growth front during crystallization. © 1998 Elsevier Science Ltd. All rights reserved.

(Keywords: isotactic polypropylene; poly(ether imide); spherulite growth)

INTRODUCTION

In a previous paper[1], an immiscibility loop in a binary mixture of isotactic polypropylene (iPP), a semi-crystalline polymer, and partially hydrogenated oligo(styrene-*co*-indene) (HSI), an amorphous oligomer, were found by the cloud point method. It is interesting to study morphology development in immiscibility loops as they are very rare in polymer blends. Morphology evolution may be expected to be different between the two phase regions inside the immiscibility and the one phase region just outside the immiscibility loop phase boundary: competition between crystallization and liquid–liquid phase separation may occur and intervene in the morphology formation, and cause a large variety of new morphologies. This motivated the study of structural formation at one phase just outside the loop and at two phases inside the loop.

The crystallization kinetics in polymer/oligomer systems is known to be non-linear; the spherulite growth rate is constant at the early stage but it decreases at the late stage. Keith and Padden[2,3] have suggested that the origin of the non-linear growth is the large mobility of the oligomer; when the oligomer can rapidly diffuse away from a growing spherulite, the concentration gradient at the growth front is established by the exclusion[4] and the spherulite growth is governed by a diffusion process[2,5,6]. In a semi-crystalline polymer/amorphous oligomer blend with immiscibility gap, the concentration gradient may cause phase change at the spherulite growth front; crystallization may induce phase separation from one phase to two phases[4] or phase dissolution from two phases to one phase. In this system, it was found that crystallization induced phase separation or phase dissolution at the growth front of the spherulite.

First, time variation of the spherulite at the two phase region inside the immiscibility loop and the one phase region just outside the loop was investigated. Then, a concentration gradient for HSI at the spherulite growth front during crystallization was quantitatively estimated and its effect on morphology formation investigated.

EXPERIMENTAL

The iPP used was a commercial polymer supplied by Mitsui Toatsu Chemicals, Inc. (J3HG; $M_w = 3.5 \times 10^5$, $M_n = 5.0 \times 10^4$). HSI was supplied by Arakawa Chemicals, Ltd (ARKON®); $M_w = 770$, styrene content = 60 wt%, degree of hydrogenation (indene) = 70%.

iPP and HSI were melt-mixed at 190°C using a Mini Max Moulder (CS-183 MMX, Custom Scientific Instruments, Inc.). The blend ratio was fixed at a 30/70 (iPP/HSI) weight ratio. The one phase melt was extruded and chopped into pellets. A thin-layer specimen (*ca.* 15 μm thick) was prepared by pressing the pellets between two cover glasses at 200°C.

The specimen was held at 200°C for a minute, and then the melt underwent a rapid quench to a crystallization temperature by putting in a hot-stage (Linkam TH600 Heating-Cooling Stage, Linkam Scientific Instruments, Ltd) set on an optical microscope stage. The time variation of the radius of iPP spherulites during isothermal annealing was observed with a polarizing optical microscope (Olympus BH-2) equipped with a TV video recording system.

The crystallization and phase separation were investigated by the time-resolved light scattering, employing the H_v (cross-polarized) and V_v (parallel-polarized) optical alignments using a CCD (charge-coupled device) camera system.

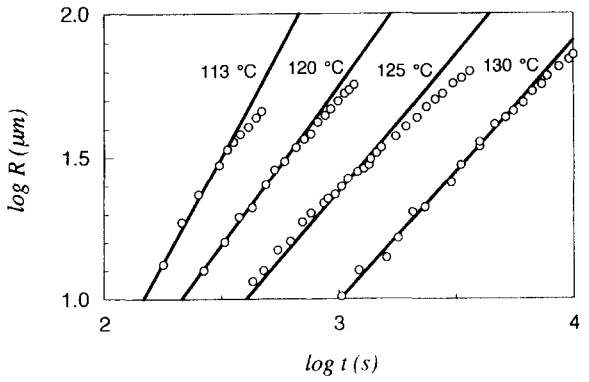

Figure 1 log R *versus* log t at various temperatures

RESULTS AND DISCUSSION

Non-linear growth of spherulite and concentration profile at its growth front

In this system the kinetics of the spherulite growth were studied. Time variations of the spherulite radius R at various temperatures are shown in *Figure 1*. R initially increases linearly with time, and later the growth rate decreases i.e. non-linear growth behaviour was found both at the two phase region inside the immiscibility loop (120, 125 and 130°C) and at the one phase region just outside the loop (113°C) (see schematic phase diagram in *Figure 7*). A typical time variation of the spherulite radius R at 130°C is shown in *Figure 2*. At this temperature, R is initially proportional to time, $R \propto t$, and later it changes to be proportional to the square root of time, $R \propto t^{1/2}$. In other words, the spherulite growth rate G (dR/dt) changes from $G \propto t^0$ (constant G) to $G \propto t^{-1/2}$: non-linear growth is seen. The transition from $G \propto t^0$ to $G \propto t^{-1/2}$ has been suggested by Cahn[7]. He formulated the growth kinetics governed by a diffusion process under a concentration gradient formed near the growth front due to the continuous segregation of oligomer.

$$\frac{dR}{dt} = \frac{(\phi_\infty - \phi_e)D/\Phi}{R_t + R} \quad (1)$$

$$R_t = D/\kappa\Phi \quad (2)$$

where ϕ_∞ is the volume fraction of the crystal component at a point far from the growth front, ϕ_e is the equilibrium volume fraction at the growth front, Φ is the volume fraction of the crystal component in the solid ($\Phi \gg \phi_e$), D is the diffusion coefficient, κ is the surface kinetic coefficient and R_t is the crossover radius at which the time variation of R begins to change from $R \propto t$ to $R \propto t^{1/2}$, as shown in *Figure 2*. For small R, equation (1) yields

$$R = [\kappa(\phi_\infty - \phi_e)]t \quad (3)$$

It implies that R is initially proportional to time, $R \propto t$. When R is large, equation (1) gives

$$R^2 = [(\phi_\infty - \phi_e)D/\Phi]t \quad (4)$$

and it corresponds to the power law of $R \propto t^{1/2}$. Thus, the change from non-linear growth to a linear may be explained by the crossover between t and $t^{1/2}$. The non-linear growth of the spherulite may induce a concentration gradient near its growing front, since the spherulite excludes the impurities (HSI)[4]. Next, the change of the concentration profile for HSI at the growth front of the spherulite is estimated quantitatively. The concentration profile at the growth front $C_{HSI}(r)$ is given by[7]

$$C_{HSI}(r) = \frac{(\phi_\infty - \phi)}{(\phi_\infty - \phi_e)} = \frac{R}{(R+r)}\frac{R}{(R+R_t)} \quad (5)$$

where r is the distance from the growth front of the spherulite.

The results of the $C_{HSI}(r)$ estimated by equation (5) are shown in *Figure 3*. It is clearly seen that $C_{HSI}(r)$ becomes higher as the spherulite grows. At an early stage (R = 12.5 μm), $C_{HSI}(r)$ shows that HSI are rejected to the outside of the spherulite but its amount is not enough to induce non-linear growth. At an intermediate stage (R_t = 42.9 μm), the rejected HSI at the growth front increase and induce non-linear growth of the spherulite: the transition from a linear growth to a non-linear one onsets. At a late stage (R =

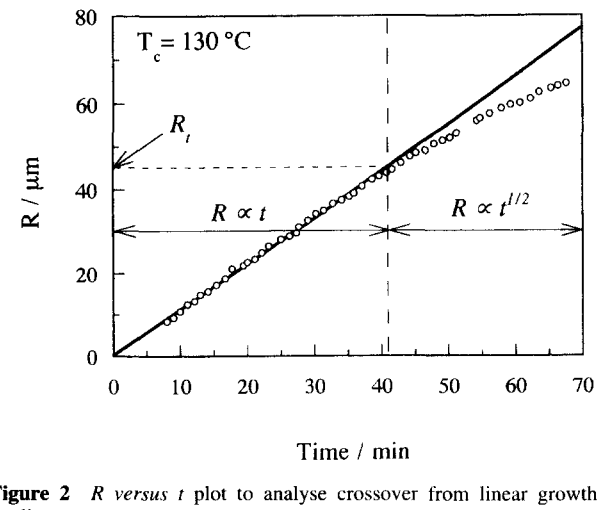

Figure 2 R *versus* t plot to analyse crossover from linear growth to nonlinear one

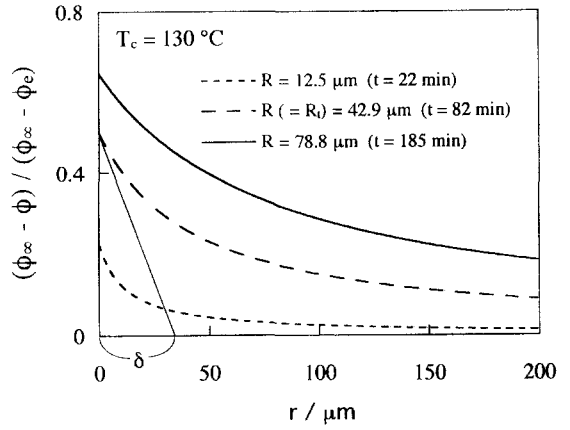

Figure 3 The change of the concentration profile for HSI at the growth front of the spherulite

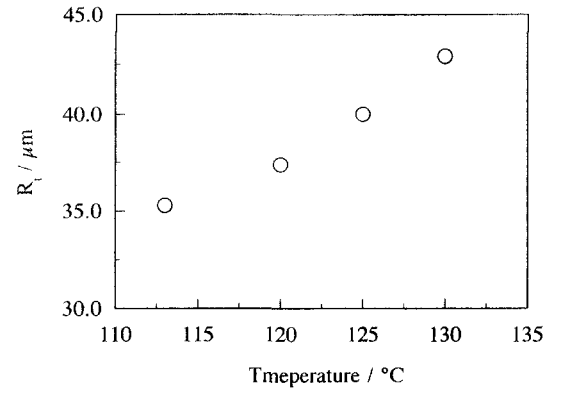

Figure 4 R_t at various temperatures

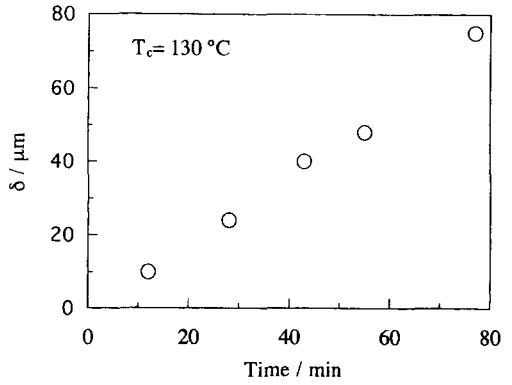

Figure 5 Time variation of the Keith–Padden's δ parameter

78.9 μm), $C_{HSI}(r)$ continues to increase with non-linear spherulite growth.

Figure 4 shows the value of R_t at various temperatures. R_t increases with increasing temperatures. It is speculated that,

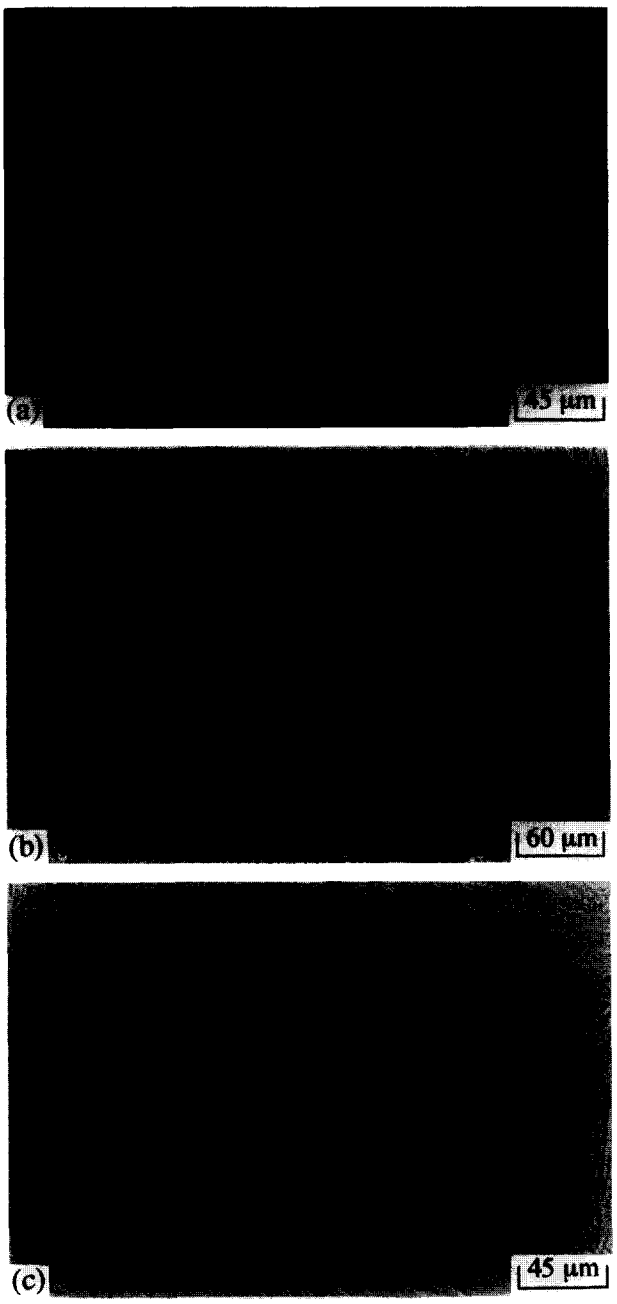

Figure 6 Optical micrographs of a 30/70 blend: (a) 12 min, (b) 43 min and (c) 180 min after temperature drop from 200 to 130°C

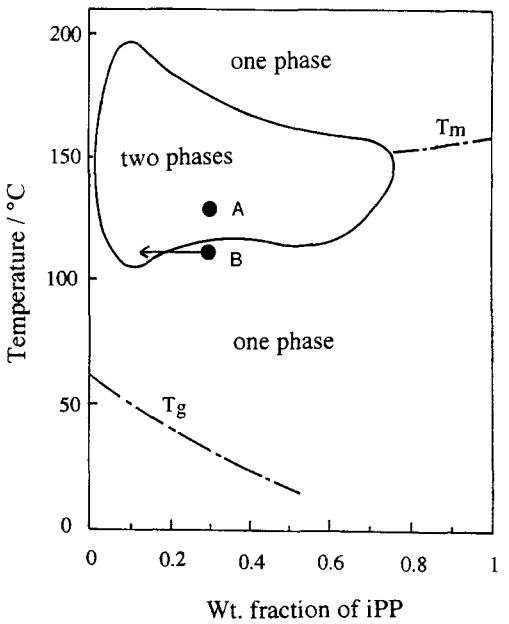

Figure 7 Schematic phase diagram of the iPP/HSI system

with increasing temperatures, the rejected HSI is easy to diffuse away due to high mobility and then sufficient HSI to induce non-linear growth is difficult to pile up at the growth front.

To discuss the effect on spherulite texture of this crystalline growth mode, it may be interesting to employ the Keith–Padden's δ parameter, which describes a scale in exclusion distance of impurities[2–9]:

$$\delta = D/G \tag{6}$$

where D is the diffusion coefficient of impurity. Originally Keith–Padden presented the parameter δ to discuss the fibril size[2,3]. Therefore the relationship between δ and spherulite texture can be investigated. As shown in *Figure 3*, the parameter δ was obtained from the position of the intercept of a continuation of the linear section of the initial slope with the x-axes[4]. The results are shown as a function of crystallization time in *Figure 5*. Though the δ values estimated are too high to discuss physical meaning on these values in detail, a general trend of the increase in δ with time is observed, implying that the fibril size increases with spherulite growth. The increase of δ may be ascribed to the decrease of G which comes from increasing the concentration of impurities at the growth front with crystallization time. The time variation of the δ can be confirmed by observing spherulite texture under optical microscopy.

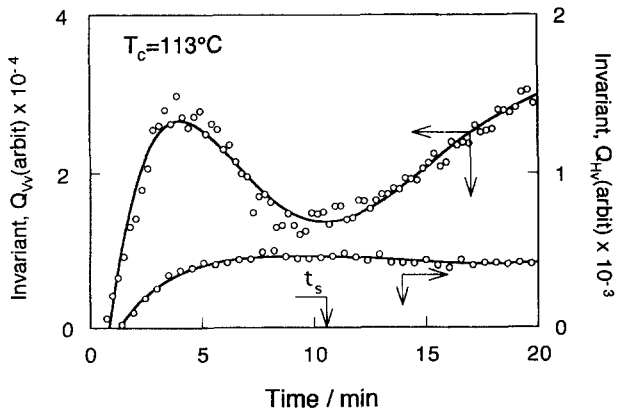

Figure 8 Time variation of the invariants Q_{Vv} and Q_{Hv} in a 30/70 iPP/HSI blend

Figure 6 shows time variation of the spherulite texture. As expected from the results discussed on δ, the fibril size in the growth front increases with spherulite growth. At the early stage, the fibril size is small (*Figure 6a*). When spherulites increase in size, the fibril size becomes larger and the outside region within spherulites shows larger fibrils (*Figure 6b*). Thus, the final spherulite (*Figure 6c*) reflects the change from the small fibril size from the rejected small HSI concentration in the early stages (centre region of the spherulite) to the large ones from the rejected high HSI concentration in the late stages (outside region within the spherulite).

Local phase change at the growth front of the spherulites

This system, iPP/HSI, has an immiscibility loop as schematically shown in *Figure 7*[1]. It is interesting to investigate morphology development at one phase region outside the loop and at two phases inside the loop. We will confine discussion to two representative temperatures; i.e. one is 113°C of the one phase region just outside the immiscibility loop (point B in *Figure 7*) and another is 130°C of the two phase region inside the loop (point A in *Figure 7*).

In this system, two sorts of phase separation are present at temperatures below T_m: liquid–liquid phase separation and crystallization. The point B is located in the one phase region just outside the immiscibility loop so that only the crystallization is expected to take place. However, after the spherulite growth proceeds to a certain level, the remaining matrix, specially the region sandwiched by the spherulites, is expected to attain the compositions inside the immiscibility loop by the rejected HSI during non-linear growth of the spherulite (see an arrow in *Figure 7*).

To discuss the crystallization process, it is convenient to employ the integrated scattering intensity, invariant Q, defined by

$$Q = \int_0^\infty I(q) q^2 \, dq \tag{7}$$

The invariant in the H_v mode, Q_{Hv}, is proportional to the mean-square optical anisotropy $\langle \delta^2 \rangle$

$$Q_{Hv} \propto \langle \delta^2 \rangle = \phi_s \delta_s^2 \tag{8}$$

where $\langle \phi_s \rangle$ is the volume fraction of spherulites and δ_s is the spherulite anisotropy[10].

On the other hand, the invariant in the V_v mode, Q_{Vv}, is ascribed to both $\langle \delta^2 \rangle$ and the mean square density fluctuation $\langle \eta^2 \rangle$. The $\langle \eta^2 \rangle$ is given by

$$\langle \eta^2 \rangle = \phi_s (1 - \phi_s)(\alpha_s - \alpha_0) \tag{9}$$

where α_s is the polarizability of the spherulite and α_0 is the polarizability of the melt.

The time variation of the invariants Q_{Vv} and Q_{Hv} after the temperature-drop from 200°C to 113°C for a 30/70 iPP/HSI mixture (point B) is shown in *Figure 8*. Q_{Hv} increases with time and then levels off, as expected from equation (8), i.e. ϕ_s increases and attains a maximum when spherulites fill the whole space. This is quite natural for polymer crystallization. Q_{Vv} increases with time, attains a maximum and then decreases. This is also expected from equation (9), since $\langle \eta^2 \rangle$ should have a maximum at $\phi_s \approx 0.5$. However, after attaining a minimum at t_s, Q_{Vv} starts to increase again. This is unexpected from equation (9). The increase after t_s should be ascribed to a new density fluctuation which is not related to crystallization, since there is no time variation in Q_{Hv} after t_s. The new density fluctuation can be assigned to the spinodal decomposition. This suggests that the matrix phase trapped between a spherulite and the adjacent ones increases the HSI concentration due to the rejected HSI during non-linear spherulite growth of the iPP, exceeds the

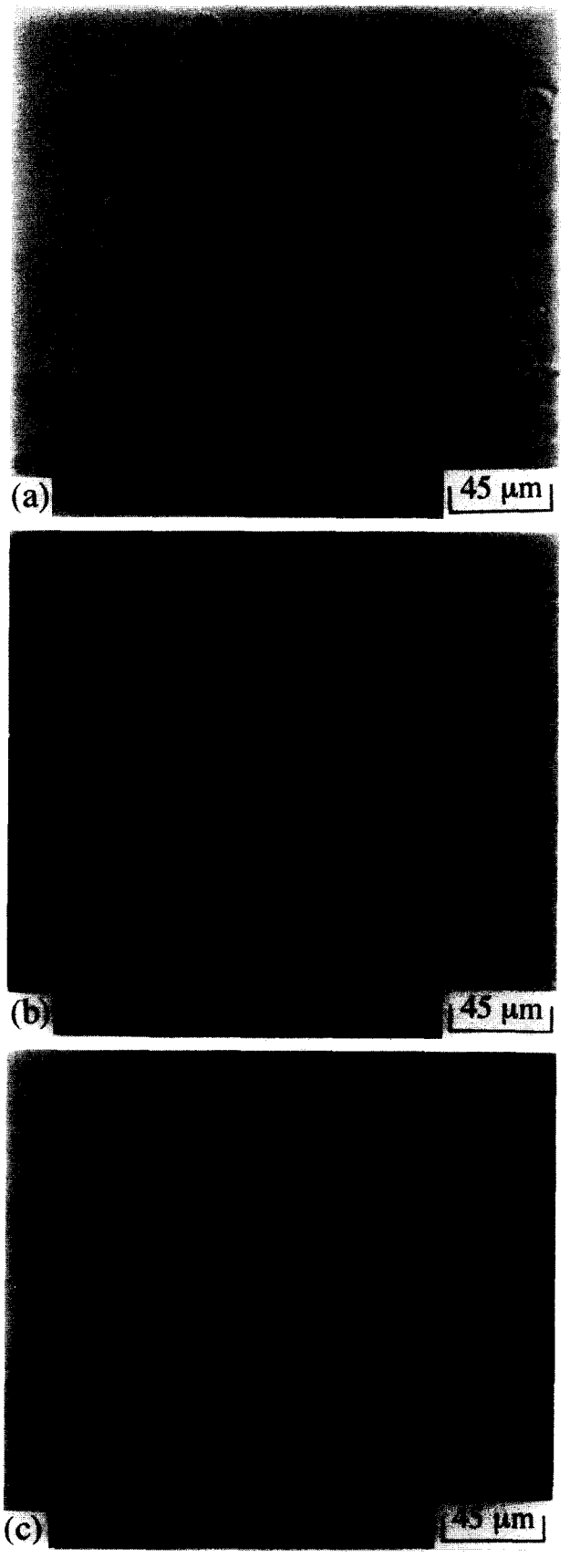

Figure 9 Optical micrographs of a 30/70 blend: (a) 3 min, (b) 18 min and (c) 25 min after temperature drop from 200 to 113°C

phase diagram line by the continuous exclusion and is thrust into the two phase region of the phase diagram (see arrow in *Figure 7*). At this temperature, structure development was observed under an optical microscope as shown in *Figure 9*. The crystallization precedes to develop the spherulites (*Figure 9a*). The spherulites grow linearly. When the spherulites change from linear growth to non-linear, the bi-continuous structure resulting from liquid–liquid phase separation appears between spherulites at the late stages of crystallization (*Figure 9b*), i.e. spinodal decomposition takes place. The impurity HSI from the spherulite can be rejected and the rejected HSI pile up at the trapped region between spherulites. This may render a mixture with the composition of the two phase region inside the immiscibility loop: crystallization induces the change from the one phase to the two phases at the matrix sandwiched between spherulites. Thus, spherulite growth should proceed from the two phases. Actually, there is memory of spinodal decomposition far from the centre of the spherulite (*Figure 9c*). The final spherulite reflects the change from the crystallization from the one phase mixture in the early stages of the spherulite growth (centre region of the spherulite) to the crystallization from the liquid–liquid phase-separated system in the late stages (outside region within the spherulite).

The microscopic observation on crystallization in the two phase region inside the immiscibility loop was investigated (point A in *Figure 7*). A 30/70 iPP/HSI blend underwent a temperature drop from 200 to 130°C, and structure development was observed under the optical microscope (see *Figure 6*). At this temperature, the spinodal decomposition proceeds to develop a regularly phase-separated bi-continuous structure followed by the spherulite formation (*Figure 6a*). The spherulites grow linearly. When the spherulites change from linear growth to non-linear, the bi-continuous structure disappears around the growing front (*Figure 6b*), i.e. dissolution of the bi-continuous structure takes place. The impurity HSI from the spherulite is rejected and the rejected HSI causes the HSI concentration profile at the growth front as shown in *Figure 3*. This may render a highly diluted mixture with the composition of the one phase region outside the immiscibility loop: crystallization induces the change from two phases to one phase at the growth front. Thus, spherulite growth should proceed from one phase. Actually, there is no memory of spinodal decomposition far from the centre of the spherulite (*Figure 6c*). The final spherulite reflects the change from the crystallization from the liquid–liquid phase-separated system in the early stages (centre region of the spherulite) to the crystallization from the one phase mixture in the late stages of the spherulite growth (outside region within the spherulite).

CONCLUSIONS

The non-linear growth behaviour in the iPP/HSI blend was demonstrated by the transition from $R \propto t$ to $R \propto t^{1/2}$. The transition was ascribed to the increased concentration of the rejected HSI at the growth front of the spherulite with crystallization. These phenomena, non-linear growth and concentration variation of HSI at growth front, were quantitatively explained by the Cahn theory. By the rejected HSI at the growth front with spherulite growth, the following arose:

(1) At 113°C just below the loop, crystallization induced the phase change from the one phase to the two phases: crystallization proceeded, it induced the liquid–liquid phase separation and then the crystallization from the two phases state took place.
(2) At 130°C inside the loop, crystallization induced the phase change from the two phases to the one phase: spinodal decomposition proceeded, the crystallization from the decomposition state followed, and then the crystallization from the one phase took place.

REFERENCES

1. Lee, C. H., Saito, H., Goizueta, G. and Inoue, T., *Macromolecules*, 1996, **29**, 4274.
2. Keith, H. D. and Padden, F. J. Jr, *J. Appl. Phys.*, 1964, **35**, 1270.
3. Keith, H. D. and Padden, F. J. Jr, *J. Appl. Phys.*, 1963, **34**, 2409.
4. Tanaka, H. D. and Nishi, T., *Phys. Rev. Lett.*, 1985, **55**, 1102.
5. Frank, F. C., *Proc. Roy. Soc.*, 1950, **A201**, 586.
6. Goldenfeld, N., *J. Crystal Growth*, 1987, **84**, 601.
7. Cahn, J. W., in *Crystal Growth*, ed. H. S. Peiser. Pergamon, New York, 1967, p. 681.
8. Keith, H. D. and Padden, F. J. Jr, *J. Polym. Sci., Part A*, 1964, **2**, 4339.
9. Stein, R. S., Khambatta, F. B., Warner, F. P., Russell, T. P., Escala, A. and Balizer, E., *J. Polym. Sci., Polym. Sym.*, 1978, **63**, 313.
10. Koberstein, T., Russell, T. P. and Stein, R. S., *J. Polym. Sci., Polym. Phys. Ed.*, 1979, **17**, 1719.